

Realization of isotropy of the lattice Boltzmann method via rotation of lattice velocity bases

Raoyang Zhang ^{*}, Ilya Staroselsky, Hudong Chen

Exa Corporation, 3 Burlington Woods Drive, Burlington, MA 01803, United States

Received 28 April 2006; received in revised form 7 December 2006; accepted 24 January 2007

Available online 9 February 2007

Abstract

We present a detailed algorithm of rotationally invariant lattice Boltzmann method (RILBM). The suggested approach overcomes discrete artifacts present in the standard lattice Bhatnagar, Gross, and Krook (LBGK) model by introducing a generalized particle collision operator in arbitrarily rotated frames. We demonstrate that the Navier–Stokes equations are exactly recovered through the Chapman–Enskog expansion, and present two computational cases that show independence of numerical results relative to the lattice orientation.

© 2007 Elsevier Inc. All rights reserved.

Keywords: Rotationally invariant lattice Boltzmann method; Navier–Stokes equations

1. Introduction

Treating continuum phenomena via discrete methods automatically involves worrying about proper control of numerical artifacts. When modeling of continuum involves just discretization in space and time of some macroscopic master equations, the available applied mathematics provides ample means to ensure that the error decreases with the finer subdivision of physical space/time. The situation is more delicate for the lattice gas (LG) and lattice Boltzmann methods (LBM) that are constructed based on a finite set of particles velocities and by that construction carry the challenge to preserve the invariance of system properties in respect to rotation of the lattice. Intuitively, the corresponding errors do not have to go away with spatial resolution, since the base set of particle velocities is always the same discrete one and certain directions are preferred. Since long time ago [1–4], it has been known how to construct smart lattice models that enforce isotropy in the limit of small mean free path λ (roughly, the lattice size) relative to the macroscopic scale L , which is of course one of the key factors allowing for successful application of lattice methods in hydrodynamics. In this paper we give in detail a description of a lattice algorithm that ensures rotational invariance for arbitrary Knudsen numbers $Kn = \lambda/L$. The conceptual framework was first presented in [5]. In addition, we provide numerical validations for some essential flow properties.

^{*} Corresponding author. Tel.: +1 781 676 8576.
E-mail address: raoyang@exa.com (R. Zhang).

The idea of the present approach is to employ the existence of a family of symmetries hidden in the construction of LBM, and indeed in any kinetic equation formulated in the configuration space. By this we mean that the coordinate system of velocity space can be defined in an absolutely arbitrary way relative to that of physical space. Such kinetic equations can be equally well formulated using any set of base vectors of velocity space, which in principle can even vary as a function of physical space and time and/or other system variables. In particular, alignment of base velocity vectors with the coordinate system of physical space in the original LG/LBM formulation is merely a convenient choice. Here, we will exploit just one possible method of variable definition of velocity space bases, namely the random rotation of a prescribed finite set, in order to construct an LBM method that is rotationally invariant for finite Kn . In this way isotropy is achieved cheap, without the necessity to increase the number of lattice speeds.

It follows that the method suggested here is another attempt to connect the discrete and the continuous descriptions, using an economical version of the former. Aside from this fundamental interest, there is a very practical motivation to develop these methods. Indeed, LBM seem to be a natural approach to micro- and nanofluidics, much more fundamental than the (generalized) Navier–Stokes (NS) equations-based and much less computationally expensive than the molecular dynamics and Monte Carlo methods. Some work using conventional LBM has already shown promise for capturing subtle high Kn flow features (cf. [6–9]). In particular the famous Knudsen effect, the non-monotonic behavior of mass flux through a pipe as a function of pressure drop, unexplainable within hydrodynamics, has been demonstrated. For the quantitative treatment of flow in complex geometries, and especially for serious engineering applications in nanodevices, the rotational invariance issue should be dealt with in a comprehensive way.

2. Rotationally invariant algorithm and hydrodynamic properties of the corresponding kinetic system

Let us start with outlining the basic concept of this approach which has been presented elsewhere [5]. The conventional lattice Boltzmann equation (LBE) is expressed in the following form:

$$f_i(\mathbf{x} + \mathbf{c}_i \Delta t, t + \Delta t) - f_i(\mathbf{x}, t) = \Omega_i(\mathbf{x}, t) \Delta t, \tag{1}$$

where $f_i(\mathbf{x}, t)$ are the distribution density functions for the particles with velocity \mathbf{c}_i , and the collision term usually takes the so called BGK form [4],

$$\Omega_i(\mathbf{x}, t) = -\frac{1}{\tau} [f_i(\mathbf{x}, t) - f_i^{\text{eq}}(\mathbf{x}, t)]. \tag{2}$$

All the hydrodynamic quantities are defined in terms of moments summation of f_i over \mathbf{c}_i :

$$\rho(\mathbf{x}, t) = \sum_{i=1}^b f_i(\mathbf{x}, t), \quad \rho \mathbf{u}(\mathbf{x}, t) = \sum_{i=1}^b \mathbf{c}_i f_i(\mathbf{x}, t), \tag{3}$$

$$\Pi_{\alpha\beta}(\mathbf{x}, t) = \sum_{i=1}^b c_{i,\alpha} c_{i,\beta} f_i(\mathbf{x}, t). \tag{4}$$

Here, ρ , \mathbf{u} , and $\Pi_{\alpha\beta}$ are macroscopic density, velocity, and momentum flux tensor, and sub-indices α and β denote Cartesian components in the D -dimensional space. In order to overcome the numerical artifacts introduced by the finite number of particle velocities, consider an ensemble of lattice velocity sets, $\mathbf{B} \equiv \{C^\beta; \beta = 1, 2, \dots, S\}$, such that all the sets have the same origin, identical crystallographic structure, but different orientations in space [5]. All the possible orientation angles are present in \mathbf{B} with equal probabilities. It is readily recognized that although each C^β is finite, the super set \mathbf{B} is in principle an infinite set. Transition between any pair of these sets, $C^\beta \leftrightarrow C^{\beta'}; \beta \neq \beta'$, can be realized through a standard rotational transformation. An extended LBE in the infinite resolution limit on a particular set C^β of the super set \mathbf{B} can be written as follows:

$$(\partial_t + \mathbf{c}_i^\beta \cdot \nabla) f_i^\beta(\mathbf{x}, t) = \Omega_i^\beta(\mathbf{x}, t); \quad \mathbf{c}_i^\beta \in \mathbf{B}. \tag{5}$$

The next step of this construction is to specify the mechanism of rotating the lattice velocities $\{\mathbf{c}^\beta\} \equiv C^\beta$. This is realized in the algorithm presented here via a transition from $C^\beta \rightarrow C^{\beta'}$ that has a set of rotated discrete velocities. In principle, for restoring rotational invariance it would suffice that all possible rotated sets are used

simultaneously, in a way that is not necessary related to the system evolution in physical time. This would introduce an extended phase space of the system, with an additional dimension that is only used to support an infinite collection of lattice orientations. However, we postulate a certain ergodicity principle [5] which says that such ensemble averaging is equivalent to averaging over orientations produced randomly in physical time. It is certainly not critical, but is just algorithmically easier, that these orientations are created at each physical time step.

Unlike in the standard LBE, arbitrarily rotated lattice velocities no longer coincide with some nodes on a given lattice. Because of that, a convenient way to treat streaming of particles is to use a volumetric propagation scheme [12]. On a lattice sub-set C^β obtained by rotating the set of standard LBE speeds by an arbitrary angle θ , particles propagate along \mathbf{c}_i^β according to the following rule:

$$f_i(\mathbf{x} \rightarrow \mathbf{x} + \Delta_i(s_x, s_y, s_z), t) = f_i^{(0)}(\mathbf{x} \rightarrow \mathbf{x} + \Delta_i(s_x, s_y, s_z), t) + f_i^{(1)}(\mathbf{x} \rightarrow \mathbf{x} + \Delta_i(s_x, s_y, s_z), t), \quad (6)$$

where

$$\Delta_i(s_x, s_y, s_z) \equiv s_x \text{sign}(\mathbf{c}_{i,x}^\beta) \Delta_x \hat{x} + s_y \text{sign}(\mathbf{c}_{i,y}^\beta) \Delta_y \hat{y} + s_z \text{sign}(\mathbf{c}_{i,z}^\beta) \Delta_z \hat{z}. \quad (7)$$

Here s_α ($\alpha = x, y, z$) take values of either 0 or 1, and \hat{x} , \hat{y} , and \hat{z} are unit Cartesian vectors. The $f_i^{(0)}$ and $f_i^{(1)}$ parts are defined as follows:

$$f_i^{(0)}(\mathbf{x} \rightarrow \mathbf{x} + \Delta_i(s_x, s_y, s_z), t) = P_x^i(s_x) P_y^i(s_y) P_z^i(s_z) \tilde{f}_i(\mathbf{x}, t), \quad (8)$$

where \tilde{f}_i denotes the “post-collide” distribution function, and

$$f_i^{(1)}(\mathbf{x} \rightarrow \mathbf{x} + \Delta_i(s_x, s_y, s_z), t) = \frac{1}{2} P_x^i(s_x) P_y^i(s_y) P_z^i(s_z) [(2s_x - 1) P_x^i(1 - s_x) G_x^i(\mathbf{x}, t) + (2s_y - 1) P_y^i(1 - s_y) G_y^i(\mathbf{x}, t) + (2s_z - 1) P_z^i(1 - s_z) G_z^i(\mathbf{x}, t)]. \quad (9)$$

Here P_α^i and G_α^i are defined as:

$$P_\alpha^i(s_\alpha) = (1 - s_\alpha) \left(1 - \frac{|\mathbf{c}_{i,\alpha}|}{\Delta_\alpha} \right) + s_\alpha \frac{|\mathbf{c}_{i,\alpha}|}{\Delta_\alpha}, \quad (10)$$

$$G_\alpha^i(\mathbf{x}, t) \equiv \tilde{f}_i(\mathbf{x} + \text{sign}(\mathbf{c}_{i,\alpha}) \Delta_\alpha \hat{\alpha}, t) - \tilde{f}_i(\mathbf{x}, t). \quad (11)$$

It has been shown in [12] that such volumetric propagation schemes exactly conserve mass and momentum while providing for a second order accurate (in time and space) realization of the following effective difference equation:

$$f_i(\mathbf{x} + \mathbf{c}_i \Delta t, t + \Delta t) = \tilde{f}_i(\mathbf{x}, t). \quad (12)$$

Since particles propagate on different lattice sets at different time steps, the collision operator not only relaxes the system towards local equilibrium, but also transits the system between different subsets C^β and $C^{\beta'}$. The challenge is to ensure preservation of correct non-equilibrium properties in such a transition process. An extended collision operator that delivers this was proposed in [5,10,11]:

$$\tilde{f}_i^\beta(\mathbf{x}, t) = f_i^{\text{eq}^\beta}(\mathbf{x}, t) + \left(1 - \frac{\Delta t}{\tau} \right) f_i^{\text{neq}^\beta}(\mathbf{x}, t), \quad (13)$$

$$f_i^{\text{neq}^\beta}(\mathbf{x}, t) = \Phi_{i,\beta}^\beta : \Phi^{\text{neq}}, \quad (14)$$

$$\Pi_{\alpha\beta}^{\text{neq}}(\mathbf{x}, t) = \sum_{i=1}^b c_{i,\alpha}^\beta c_{i,\beta}^{\beta'} [f_i^{\beta'}(\mathbf{x}, t) - f_i^{\text{eq}^{\beta'}}(\mathbf{x}, t)], \quad (15)$$

$$\Phi_{i,\alpha\beta}^\beta = \frac{w_i}{2T_0} \left[\frac{c_{i,\alpha}^\beta c_{i,\beta}^\beta}{T_0} - \delta_{\alpha\beta} \right]. \quad (16)$$

Here, T_0 is the so called lattice temperature (e.g. $T_0 = 1/3$ in D3Q19) [13,14] and $\Pi_{\alpha\beta}^{\text{neq}}(\mathbf{x}, t)$ is the pre-transformed non-equilibrium part of momentum flux. The operator $\Phi_{i,\alpha\beta}^\beta$ serves to project the system's properties onto the transformed set C^β in such a way that momentum flux between the pre- and post-transformed lattice

sets ($C^{\beta'} \rightarrow C^{\beta}$) is preserved. The equilibrium distribution function $f_i^{\text{eq}\beta}(\mathbf{x}, t)$ has the standard form up to the third order in the post-transformed lattice set C^{β} [14]:

$$f_i^{\text{eq}\beta} = w_i \rho \left[1 + \frac{\mathbf{c}_i^{\beta} \cdot \mathbf{u}}{T_0} + \frac{(\mathbf{c}_i^{\beta} \cdot \mathbf{u})^2}{2T_0^2} - \frac{\mathbf{u}^2}{2T_0} + \frac{(\mathbf{c}_i^{\beta} \cdot \mathbf{u})^3}{6T_0^3} - \frac{\mathbf{c}_i^{\beta} \cdot \mathbf{u}}{2T_0^2} \mathbf{u}^2 \right]. \tag{17}$$

This distribution function is easily constructed using ρ and \mathbf{u} obtained from the pre-transformed distributions just because the transformation of lattice velocity bases introduced here leaves these hydrodynamic quantities invariant.

It is straightforward to also show that the non-equilibrium part of the extended collision operator conserves mass and momentum as well as preserves the non-equilibrium momentum flux tensor. The latter is essential to recover the same shear viscosity as in the standard LBGK:

$$\sum_i f_i^{\text{neq}\beta} \rightarrow \sum_i w_i \left(\frac{c_{i,\alpha}^{\beta} c_{i,\gamma}^{\beta}}{T_0} - \delta_{\alpha\gamma} \right) = 0, \tag{18}$$

$$\sum_i c_{i,\alpha}^{\beta} f_i^{\text{neq}\beta} \rightarrow \sum_i w_i \left(\frac{c_{i,\alpha}^{\beta} c_{i,\gamma}^{\beta} c_{i,\theta}^{\beta}}{T_0} - c_{i,\alpha}^{\beta} \delta_{\gamma\theta} \right) = 0. \tag{19}$$

The preservation of momentum flux follows from satisfying the following condition

$$\sum_i \mathbf{c}_i \mathbf{c}_i f_i^{\text{neq}} = \sum_i \mathbf{c}_i \mathbf{c}_i (f_i - f_i^{\text{eq}}). \tag{20}$$

Indeed, from Eq. (14) we have:

$$\sum_i \mathbf{c}_i \mathbf{c}_i f_i^{\text{neq}} = \sum_i \frac{1}{2T_0^2} w_i \mathbf{c}_i \mathbf{c}_i [\mathbf{c}_i \mathbf{c}_i - T_0 \mathbf{I}] : \sum_j \mathbf{c}_j \mathbf{c}_j (f_j - f_j^{\text{eq}}) \tag{21}$$

$$= \frac{1}{2T_0^2} \sum_i w_i [\mathbf{c}_i \mathbf{c}_i \mathbf{c}_i \mathbf{c}_i - T_0 \mathbf{c}_i \mathbf{c}_i \mathbf{I}] : \sum_j \mathbf{c}_j \mathbf{c}_j (f_j - f_j^{\text{eq}}). \tag{22}$$

Upon observing that lattice velocity vectors of a standard LBM, such as LBGK, deliver the fourth order isotropy [1,5],

$$\sum_i w_i \mathbf{c}_{i,\alpha} \mathbf{c}_{i,\beta} \mathbf{c}_{i,\gamma} \mathbf{c}_{i,\theta} = \sum_i w_i \frac{\mathbf{c}_i^4}{D(D+2)} (\delta_{\alpha\beta} \delta_{\gamma\theta} + \delta_{\alpha\gamma} \delta_{\beta\theta} + \delta_{\alpha\theta} \delta_{\beta\gamma}), \tag{23}$$

and noting that

$$\sum_i w_i \mathbf{c}_{i,\alpha} \mathbf{c}_{i,\beta} = T_0 \delta_{\alpha\beta}, \tag{24}$$

the validity of Eq. (20) is readily established.

The finite volume-based advection process combined with the extended collision process outlined above define algorithmically the rotationally invariant lattice system suggested here. It is now important to show that the formulation of momentum flux according to Eqs. (14)–(16) gives rise to the same viscosity as in the standard LBGK. In the continuum limit, the effective difference Eq. (12) reduces, at the leading order, to the following equation:

$$\Delta t (\partial_t + \mathbf{c}_i \cdot \nabla) f_i = f_i^{\text{eq}} - f_i + \left(1 - \frac{\Delta t}{\tau} \right) f_i^{\text{neq}}. \tag{25}$$

Using the Chapman–Enskog expansion [15],

$$f_i = f_i^{\text{eq}} + f_i^{(1)} + \dots, \tag{26}$$

the zeroth order of Eq. (25) becomes

$$\Delta t (\partial_t + \mathbf{c}_i \cdot \nabla) f_i^{\text{eq}} = -f_i^{(1)} + \left(1 - \frac{\Delta t}{\tau} \right) f_i^{\text{neq}}. \tag{27}$$

Due to the vanishing right hand side, the momentum Eq. (25) is immediately obtained:

$$\sum_i \mathbf{c}_i (\partial_t + \mathbf{c}_i \cdot \nabla) f_i = \partial_t (\rho \mathbf{u}) + \nabla \cdot \sum_i \mathbf{c}_i \mathbf{c}_i f_i = 0, \quad (28)$$

and from (27) the leading order momentum flux equation can be written as:

$$\Delta t \sum_i \mathbf{c}_i \mathbf{c}_i (\partial_t + \mathbf{c}_i \cdot \nabla) f_i^{\text{eq}} = - \sum_i \mathbf{c}_i \mathbf{c}_i f_i^{(1)} + \left(1 - \frac{\Delta t}{\tau}\right) \sum_i \mathbf{c}_i \mathbf{c}_i f_i^{\text{neq}}. \quad (29)$$

By noting that $f_i^{(1)} = f_i - f_i^{\text{eq}}$ and using Eq. (20), Eq. (29) is reduced to it's familiar form:

$$\sum_i \mathbf{c}_i \mathbf{c}_i (\partial_t + \mathbf{c}_i \cdot \nabla) f_i^{\text{eq}} = - \frac{1}{\tau} \sum_i \mathbf{c}_i \mathbf{c}_i f_i^{(1)}. \quad (30)$$

Hence the momentum Eq. (28) can be written as

$$\partial_t (\rho \mathbf{u}) + \nabla \cdot \left[\sum_i \mathbf{c}_i \mathbf{c}_i f_i^{\text{eq}} + \sum_i \mathbf{c}_i \mathbf{c}_i f_i^{(1)} \right] = \partial_t (\rho \mathbf{u}) + \nabla \cdot \left[\sum_i \mathbf{c}_i \mathbf{c}_i - \tau \sum_i \mathbf{c}_i \mathbf{c}_i (\partial_t + \mathbf{c}_i \cdot \nabla) \right] f_i^{\text{eq}} = 0. \quad (31)$$

Eq. (31) has exactly the same expanded form as that of the standard LBGK. This means that the generalized collision operator formulated above exactly recovers the same NS equations as LBGK does, with the same viscosity equal to

$$\nu = (\tau - \Delta t/2) T_0.$$

Furthermore, since the definition of momentum flux is

$$\sum_i \mathbf{c}_i \mathbf{c}_i (\tilde{f}_i - f_i) = - \sum_i \mathbf{c}_i \mathbf{c}_i (f_i - f_i^{\text{eq}}) + \left(1 - \frac{\Delta t}{\tau}\right) \sum_i \mathbf{c}_i \mathbf{c}_i f_i^{\text{neq}}, \quad (32)$$

using Eq. (20) we obtain

$$\sum_i \mathbf{c}_i \mathbf{c}_i (\tilde{f}_i - f_i) = - \frac{\Delta t}{\tau} \sum_i \mathbf{c}_i \mathbf{c}_i (f_i - f_i^{\text{eq}}). \quad (33)$$

By noticing that the right side of this equation is just the definition of momentum flux in LBGK, we again show the momentum flux is exactly the same as that of the LBGK. Let us emphasize that all these “standard” features are now obtained in a potentially much more powerful algorithm satisfying invariance under any lattice rotations.

In summary, the fully rotational invariant LBM approach (RILBM) presented here consists of the following steps:

- (1) Advect the distribution functions on a specific lattice subset C^β using volumetric propagation;
- (2) Calculation of the post-advect mass, momentum, and stress tensor from C^β ;
- (3) Generate a new lattice subset $C^{\beta'}$ by an arbitrary rotation of the existing C^β ;
- (4) Transform the distribution functions from C^β to $C^{\beta'}$ via applying the extended collision operator (13) that preserves both the equilibrium and non-equilibrium moments and relax (by τ) the distribution functions towards local equilibrium on the new lattice subset $C^{\beta'}$.

Below we discuss simulation data that provide support for some of the theoretical arguments presented in this section. Note that this numerical verification is only possible because RIBLM allows an efficient algorithmic formulation outlined above.

3. Numerical results

The first test case is a simulation of sinusoidal wave decay involving two distinct orientations. One has the wave vector oriented along a lattice aligned direction in a square domain, and another is realized via a 45°

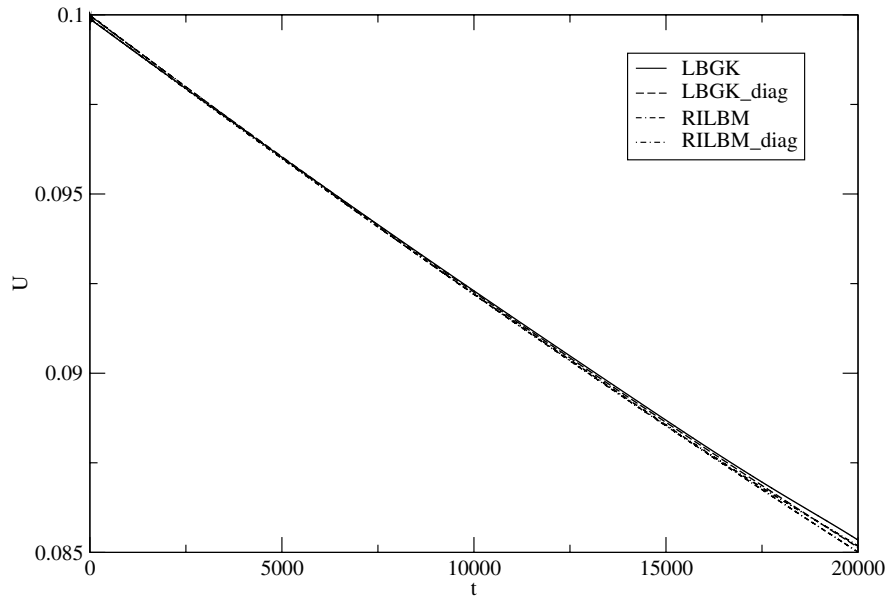


Fig. 1. Comparison of sinusoidal wave decay rate at $Kn = 0.00028/2\pi$. Curves with the subscript “diag” refer to the simulation results corresponding to the 45° rotation of the computational domain.

rotation in a tilted square domain. Dimensions of the aligned and the tilted square are (128×128) and (181×181) , respectively. The wave numbers $K (\equiv 2\pi/128)$ for the simulated sinusoidal waves and other flow quantities in these two different setups are designed to be equal. Clearly, if a system is lattice orientation-invariant, decay rates for the two different setups should be the same for all Knudsen numbers $Kn = c_s \tau K / 2\pi$. As mentioned above, the fluid flow is within the NS regime when $Kn \ll 1$. In Fig. 1 we plot

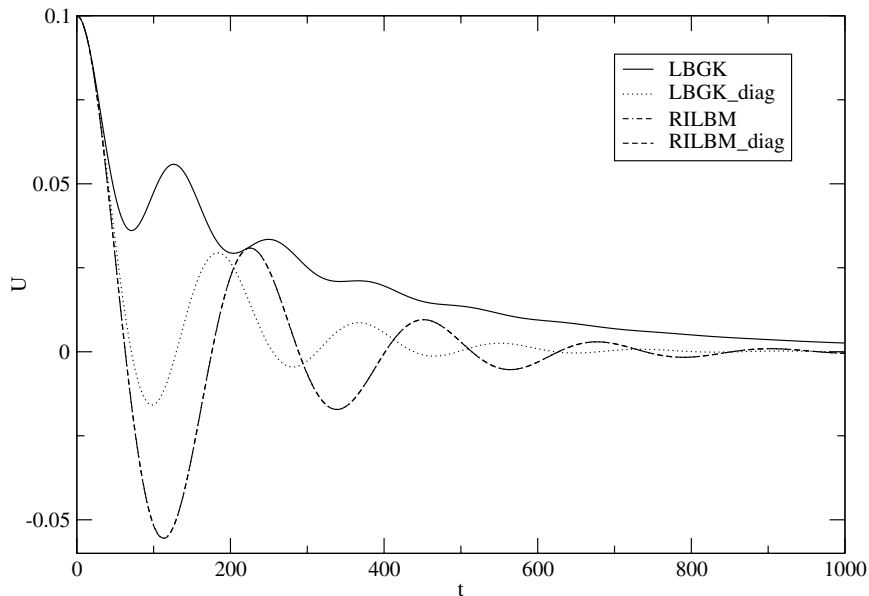


Fig. 2. Comparison of sinusoidal wave decay rate at $Kn = 2.8/2\pi$. Curves with the subscript “diag” refer to the simulation results corresponding to the 45° rotation of the computational domain. Note that curves corresponding to the RILBM and RILBM_diag results are both present in this plot, but not visually distinguishable.

simulation results at $Kn = 0.00028/2\pi$. Results given by LBGK and RILBM for both the aligned and tilted orientations are very close to each other. This indicates that, as expected, RILBM is as accurate as LBGK in the NS regime and the decay rates given by both methods are not sensitive to the lattice rotation. On the other hand, in Fig. 2 we plot the results for $Kn = 2.8/2\pi$. Because of the sufficient isotropy of RILBM, it gives the same results for the two different lattice orientations while the LBGK results show a strong lattice orientation dependence.

The second test case involves sound wave propagation. At the center point of a two dimensional square simulation domain, the initial value of density (pressure) is set to one percent higher than that in the surrounding fluid. Physically, this perturbation should propagate at the speed of sound $c_s = \sqrt{T_0}$ with a circular front in all directions, before approaching the square simulation domain boundary. Due to the discrete rotation artifacts, the circular sound wave propagation is not expected in a standard LBM at high Kn , even when the front is far from the domain boundary.

Fig. 3 shows a comparison of sound wave propagation simulated using LBGK and RILBM at $Kn = c_s\tau/L = 0.00005$. At this small Kn , both schemes give satisfactory results. The images represent pressure distributions. Similar to the shear wave decay case, it is understood that the conventional LBGK is isotropic

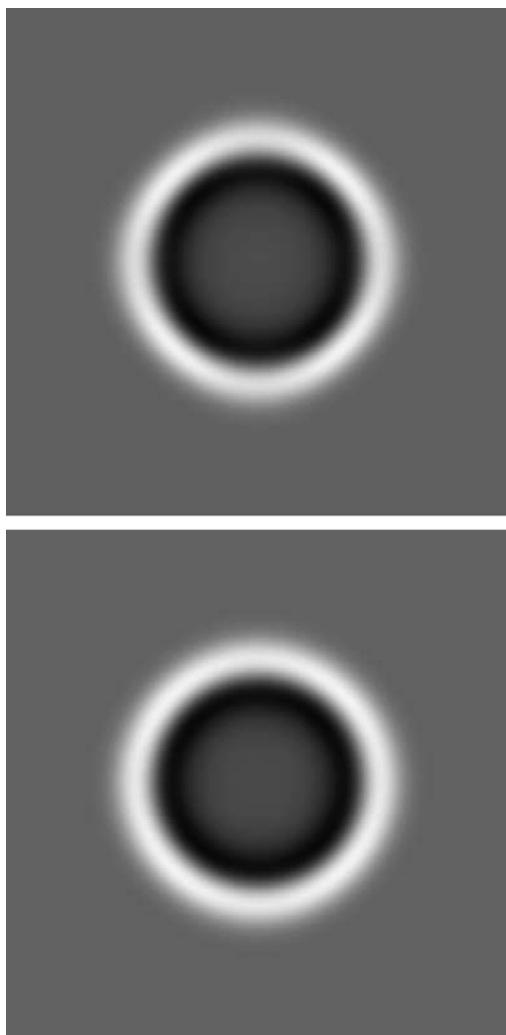


Fig. 3. Comparison of sound wave propagation at $Kn = 0.00005$. The upper and bottom plots correspond to the LBGK and the RILBM results, respectively.

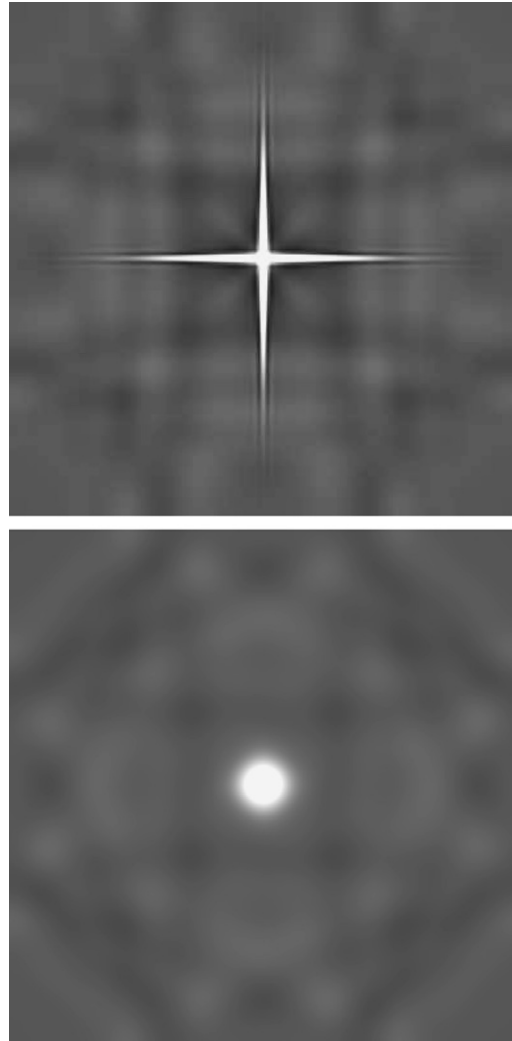


Fig. 4. Comparison of sound wave propagation at $Kn = 0.5$. The upper and bottom plots correspond to the LBGK and the RILBM results, respectively.

up to the NS order and is thus able to capture the circular sound wave propagation within the NS regime. However, as shown in Fig. 4, the situation becomes different at $Kn = 0.5$, well beyond the NS regime. As expected, the conventional LBGK fails to predict circular sound wave propagation due to having preferred lattice directions. At the same time, RILBM preserves the isotropic sound wave front at all times.

4. Discussion

In this paper we present in detail an efficient lattice algorithm, suggested earlier in [5], that achieves full rotational invariance with respect to lattice orientations. As discussed in [5], LBGK suffers from discrete orientation artifacts at finite Kn as a result of employing a finite set of lattice velocities. This intrinsic defect is a consequence of a finite set of discrete velocities, and is independent of temporal and spatial resolution. RILBM uses an “infinite” set of lattice velocities that “densely covers” the continuum of lattice directions via random rotations at each simulation time step. In the limit of infinite temporal or spatial resolution, RILBM is expected to be fully rotationally invariant. Algorithmic implementation of this scheme is possible and described, and the numerical results provide direct support for the theoretical predictions given above in

this manuscript as well as in [5]. In the future, we are planning to investigate more cases of various nature, especially those with strong nonlinearity (c.f. [16]), concerning boundary conditions (c.f. [17–19]), including also three dimensional situations, as well as involve certain extensions of the underlying lattice models [20]. We wish to stress that RILBM and its complete algorithm is applicable to all flow situations, albeit linear or nonlinear.

Finally, we would like to emphasize an essential difference between the functionality of collision operators in the standard LBGK and our RILBM. The LBGK contains non-equilibrium moments of all orders, which however are not necessarily isotropic, hydrodynamic, or physically meaningful. The projection operator in RILBM extracts the non-equilibrium properties at the momentum moment order only. In other words, RILBM only preserves and relaxes the modes of interest while the non-equilibrium properties associated with the other modes are destroyed. It is known that this is sufficient and desirable for recovery of the Navier–Stokes order fluid physics [1,2,5]. On the other hand, by extending the projection operator to include additional moments, high order non-equilibrium information essential for high Kn regimes can be realized [11,20]. Furthermore, such a regularization of the non-equilibrium part of particle distribution functions should significantly improve flow results at high Kn regimes.

Acknowledgment

This work was partially supported by the NSF.

References

- [1] S. Wolfram, Cellular automation fluids.1. Basic theory, *J. Stat. Phys.* 45 (1986) 471.
- [2] U. Frisch et al., Lattice gas hydrodynamics in two and three dimensions, *Complex Syst.* 1 (1987) 649–707.
- [3] R. Benzi, S. Succi, M. Vergassola, The lattice Boltzmann-equation – theory and applications, *Phys. Rep.* 222 (1992) 145.
- [4] S. Chen, G. Doolen, Lattice Boltzmann method for fluid flows, *Annu. Rev. Fluid Mech.* 30 (1998) 329.
- [5] H. Chen, R. Zhang, I. Staroselsky, M. Jhon, Recovery of full rotational invariance in lattice Boltzmann formulations for high Knudsen number flows, *Physica A* 362 (1) (2006) 125.
- [6] K. Xu, Super-Burnett solutions for Poiseuille flow, *Phys. Fluids* 15 (7) (2003) 2077.
- [7] F. Toschi, S. Succi, Lattice Boltzmann method at finite Knudsen numbers, *Europhys. Lett.* 6944 (2005) 549.
- [8] Y. Zhou, R. Zhang, I. Staroselsky, H. Chen, W.T. Kim, M. Jhon, Simulation of micro- and nano-scale flows via the lattice Boltzmann method, *Physica A* 362 (1) (2006) 68.
- [9] X. Nie, G. Doolen, S. Chen, Lattice-Boltzmann simulations of fluid flows in MEMS, *J. Stat. Phys.* 107 (1–2) (2002) 279.
- [10] J. Latt, B. Chopard, Lattice Boltzmann method with regularized pre-collision distribution functions, *Math. Comput. Simulat.* 72 (2–6) (2006) 165.
- [11] R. Zhang, X. Shan, H. Chen, Efficient kinetic method for fluid simulation beyond the Navier–Stokes equation, *Phys. Rev. E* 74 (4) (2006) 046703.
- [12] H. Chen, Volumetric formulation of the lattice Boltzmann method for fluid dynamics: basic concept, *Phys. Rev. E* 58 (1998) 3955.
- [13] Y.H. Qian, d’Humières, P. Lallemand, Lattice BGK models for Navier–Stokes equation, *Europhys. Lett.* 17 (1992) 479.
- [14] H. Chen, C. Teixeira, K. Molvig, Digital physics approach to computational fluid dynamics: some basic theoretical features, *Int. J. Mod. Phys. C* 8 (4) (1997) 675;
H. Chen, C. Teixeira, H-theorem and origins of instability in thermal lattice Boltzmann models, *Comput. Phys. Commun.* 129 (2000) 21.
- [15] S. Chapman, T. Cowling, *The Mathematical Theory of Non-Uniform Gases*, third ed., Cambridge University Press, Cambridge, 1990.
- [16] H. Fan, R. Zhang, H. Chen, Extended volumetric scheme for lattice Boltzmann models, *Phys. Rev. E* 73 (6) (2006) 066708.
- [17] S. Ansumali, I. Karlin, Kinetic boundary conditions in the lattice Boltzmann method, *Phys. Rev. E* 66 (2) (2002) 026311.
- [18] M. Sbragaglia, S. Succi, Analytical calculation of slip flow in lattice Boltzmann models with kinetic boundary conditions, *Phys. Fluids* 17 (9) (2005) 093602.
- [19] H. Chen, C. Teixeira, K. Molvig, Realization of fluid boundary conditions via discrete Boltzmann dynamics, *Int. J. Mod. Phys. C* 9 (8) (1998) 1281.
- [20] X. Shan, X.-F. Yuan, H. Chen, Kinetic theory representation of hydrodynamics: a way beyond the Navier–Stokes equation, *J. Fluid Mech.* 550 (2006) 413.